OXFORD

RESEARCH ARTICLE

# Knockdown of Dopamine $D_2$ Receptors in the Nucleus Accumbens Core Suppresses Methamphetamine-Induced Behaviors and Signal Transduction in Mice

Yoshiaki Miyamoto, PhD; Asako Iida, MSc; Keiji Sato, BSc;
Shin-ichi Muramatsu, MD, PhD; Atsumi Nitta, PhD

Department of Pharmaceutical Therapy and Neuropharmacology, Faculty of Pharmaceutical Sciences, Graduate School of Medicine and Pharmaceutical Sciences, University of Toyama, Toyama, Japan (Drs Miyamoto, Sato, and Nitta); [2]Division of Neurology, Department of Medicine, Jichi Medical University, Tochigi, Japan (Drs Iida and Muramatsu).

Correspondence: Atsumi Nitta, PhD, Department of Pharmaceutical Therapy and Neuropharmacology, Faculty of Pharmaceutical Sciences, Graduate School of Medicine and Pharmaceutical Sciences, University of Toyama, 2630 Sugitani, Toyama, Toyama 930-0194, Japan (nitta@pha.u-toyama.ac.jp).

## Abstract

**Background:** Addictive drugs lead to reinforcing properties by increasing dopamine in the nucleus accumbens, which is composed of a core and shell regions. Neurons in the nucleus accumbens are divided into 2 subtypes based on the differential gene expression of the dopamine $D_1$ receptors and $D_2$ receptors.

**Methods:** In the present study, we investigated the role of $D_2$ receptors in the nucleus accumbens core in behaviors and signal transduction induced by psychostimulant methamphetamine in mice that were microinjected with adeno-associated virus vectors containing a microRNA (miRNA) sequence for $D_2$ receptor (adeno-associated virus-mi$D_2$r vectors) in the nucleus accumbens core. The adeno-associated virus vectors containing a miRNA sequence for $D_2$ receptor-treated mice (mi$D_2$r mice) were assessed at a reduction in $D_2$ receptor, but at no change in dopamine $D_1$ receptor, in the nucleus accumbens core compared with the adeno-associated virus-Mock vectors-treated mice (Mock mice).

**Results:** mi$D_2$r mice exhibited a reduction in hyperlocomotion that was induced by a single treatment with methamphetamine. The development of locomotor sensitization induced by repeated treatment with methamphetamine exhibited less extension in mi$D_2$r mice. In a place conditioning paradigm, the preferred effects of methamphetamine were significantly weaker in mi$D_2$r mice than in Mock mice. Furthermore, the single treatment with methamphetamine-induced phosphorylation of extracellular signal regulated kinase and cyclic adenosine monophosphate response element-binding protein in the nucleus accumbens core of mi$D_2$r mice was decreased compared with that in Mock mice. Repeated treatment with methamphetamine-induced delta FBJ murine osteosarcoma viral oncogene homolog B accumulation in the nucleus accumbens core of mi$D_2$r mice was also attenuated.

**Conclusions:** These findings suggest that a $D_2$ receptor-mediated neuronal pathway from the nucleus accumbens core plays an inhibitory role in the development of reinforcing properties.

**Keywords:** adeno-associated virus vectors, dopamine $D_2$ receptors, nucleus accumbens, methamphetamine

## Introduction

Addictive drugs, such as methamphetamine (METH; derivative of amphetamine, *N*-metyl-amphetamine), cocaine, nicotine, and morphine mediate their reinforcing properties by targeting the mesolimbic neuronal system. This neuronal system is a major dopamine (DA) pathway in the brain and originates from the ventral tegmental area (VTA) of the midbrain and projects to the nucleus accumbens (NAc), amygdala, hippocampus, and prefrontal cortex. In particular, the VTA-NAc pathway plays a critical role in mediating the reinforcing properties of drugs of abuse (Hyman et al., 2006). Although addictive drugs differ in their primary molecular targets, they consequently lead to a common event in which extracellular DA levels are directly or indirectly increased in the NAc (Lüscher and Ungless, 2006). Therefore, in the synaptic terminals of DA neurons in the NAc, METH promotes nonvesicular release and cocaine acts as an inhibitor of the DA transporter. In the VTA of the VTA-NAc pathway, nicotine directly depolarizes DA neurons, whereas morphine indirectly affects them via presynaptic inhibition of inhibitory interneurons (i.e., disinhibition of DA neurons).

Almost all the neurons in the NAc are γ-aminobutyric acid-productive medium spiny neurons (MSNs). The NAc is anatomically divided into a core region, which surrounds the anterior commissure, and a shell region, which is located in the rostral pole of the extended amygdala. The former is distinguished from the latter by differences in staining density for a number of neuropeptides, such as substance P, dynorphin, and enkephalin (Groenewegen et al., 1999). Furthermore, the NAc neurons are divided into 2 major populations on the basis of their distinct projections through differential gene expression, a direct pathway from MSNs, expressing dopamine $D_1$ receptors ($D_1$rs), and an indirect pathway from MSNs, expressing dopamine $D_2$ receptors ($D_2$rs) (Kreitzer and Malenka, 2008). The $D_1$rs are coupled to Golf and/or Gs proteins, which, on activation, stimulate adenylyl cyclase, promote the formation of cyclic adenosine monophosphate (cAMP), and activate protein kinase A (PKA), whereas $D_2$rs are coupled to Gi proteins, which inhibit the formation of cAMP, thereby decreasing PKA activity (Stoof and Kebabian, 1981; Missale et al., 1998). Both receptors in MSNs can also differentially regulate intracellular signal transduction such as the extracellular signal regulated kinase (ERK), dopamine and camp-regulated phosphoprotein of 32 kDa, and cAMP response element-binding protein (CREB) cascades. The direct pathway originates from $D_1$rs-expressing MSNs in the core region of the NAc that project to the lateral division of the VTA and the medial division of the substantia nigra pars compacta output nuclei. The indirect pathway originates from $D_2$rs-expressing MSNs in the core region of the NAc that project to the substantia nigra pars reticulata (SNr) and the dorsolateral division of the ventral pallidum, which together with the subthalamic nucleus contain trans-synaptic circuits connecting to the basal output nuclei (Humphries and Prescott, 2010).

The direct and indirect pathways from the dorsal striatum (dSTR) provide contrasting regulation of the basal ganglia output interface (Gerfen and Surmeier, 2011). However, little is known about the specific function of the 2 major populations of the NAc projection neurons. In the present study, to investigate the functional role of the indirect pathway from MSNs expressing $D_2$rs in addictive properties, we examined behaviors and signal transduction in response to METH in $D_2$rs knockdown mice that were delivered adeno-associated virus (AAV) containing a microRNA (miRNA) sequence for $D_2$r in the NAc core.

## Materials and Methods

### Animals

Male C57BL/6J mice (Nihon SLC, Hamamatsu, Japan) were 8 weeks old and weighed 22 to 27 g at the beginning of the experiments. The animals were housed in plastic cages and kept in a regulated environment (24±1ºC, 50±5% humidity) with a 12-h–light/–dark cycle (lights on at 8:00 ᴀᴍ). Food and water were available ad libitum. All experiments followed the National Institute of Health Guidelines for the Care and Use of Laboratory Animals and were approved by the committee for Animal Experiments of University of Toyama.

### Drugs and Antibodies

METH HCl was purchased from Dainippon Pharmaceutical Co., Ltd. (Osaka, Japan) and dissolved in sterile saline. Anti-$D_2$r or anti-green fluorescent protein (GFP) antibodies were obtained from Abcam (Cambridge, UK). Anti-$D_1$r antibody was obtained from Sigma-Aldrich (St. Louis, MO). Antibodies against phospho-ERK1/2 (Threonine 202/Tyrosine 204), ERK1/2, phospho-CREB (Serine 133), CREB, delta FBJ murine osteosarcoma viral oncogene homolog B (FosB), and β-tubulin were purchased from Cell Signaling Technology (Danvers, MA). Other agents were obtained from standard commercial sources.

### Production of AAV Vectors

We generated AAV vectors based on a previous report (Krzyzosiak et al., 2010). In brief, we used a vector plasmid containing an expression cassette in which a human cytomegalovirus immediate-early promoter was followed by the first intron of the human growth hormone gene, cDNA of interest, woodchuck hepatitis virus posttranscriptional regulatory element (nucleotides 1093–1684, GenBank accession number J04514) and simian virus 40 polyadenylation signal sequence. This expression cassette was inserted between the inverted terminal repeats of the AAV2 genome as previously described (Li et al., 2006). The viral vector was designed to express an antisense sequence for the $D_2$r (TTCACTGGGAAACTCCCATTA) and enhanced Gfp sequence (AAV-mi$D_2$r vectors) based on murine miR-155 (BLOCK-iT, Invitrogen). Viral vectors containing only the enhanced GFP sequence (AAV-Mock vectors) were used as a control. We used 2 helper plasmids, pAAV-RC and pHelper, harboring the AAV2 rep and cap genes and E2A, E4, and VA1 genes of the adenovirus genome, respectively (Agilent Technologies, Santa Clara, CA). HEK293 cells were cotransfected with the pAAV-RC and pHelper plasmids using the calcium phosphate coprecipitation method. AAV particles were then harvested and purified by 2 sequential continuous CsCl ultracentrifugations. The vector titer was determined by quantitative polymerase chain reaction (PCR) of the DNase-I-treated vector stocks and was estimated at $10^{11}$ to $10^{12}$ vector genome copies.

### Microinjection of AAV Vectors

Naive mice were anesthetized with pentobarbital sodium (50 mg/kg, intraperitoneally). The animals received a single bilateral microinjection of the AAV-mi$D_2$r or AAV-Mock vectors (each 0.7 μL/side) into the NAc (bregma=+1.4; lateral=±0.6; ventral=+4.2 mm position in the Mouse Brain Atlas; Franklin and Paxinos, 2007) using a stereotaxic apparatus. The injection was performed at 0.05 μL/min through a syringe with a 33-gauge needle (Hamilton, Reno, NV), and the syringe needle was left in place for an additional 15 minutes. The mice were used for the experiments 3 weeks later.

## Quantitative RT-PCR

Mice were sacrificed by cervical dislocation. Whole brains were removed and divided into 1-mm–thick sections using a mouse brain matrix (Neuroscience, Tokyo, Japan). Tissue corresponding to the NAc was collected with a 2-mm punch from the section. Likewise, the dSTR tissue was collected using a 2-mm punch from the subsequent section. The accurate locations of these brain structures were based on visual inspection of each section using a stereomicroscope and its comparison with the stereotaxic atlas of the mouse brain (Franklin and Paxinos, 2007). Tissue samples were placed on dry ice and maintained at –80°C until use. Total RNA extraction was performed using the RNeasy Plus Mini Kit (QIAGEN, Valencia, CA). Total RNA from each tissue sample was transcribed into cDNA using the PrimeScript RT reagent Kit (Takara, Shiga, Japan) according to the manufacturer's recommendations. In brief, the reaction was performed at 37°C for 20 minutes in a total volume of 10 μL and inactivated at 85°C for 5 seconds. Twenty-times diluted cDNA was used as a template, and quantitative real-time PCR was run in the Thermal Cycler Dice Real Time System (Takara) using the Power SYBR Green PCR Master Mix (Applied Biosystems, Foster, CA) with cDNA and gene-specific primers (1 μM) according to the manufacturer's instructions. All the reactions were performed in duplicate with the following cycling protocol: 10 minutes of heat activation of the enzyme at 95°C, 45 cycles of denaturation at 95°C for 5 seconds, annealing at 60°C for 30 seconds, and extension at 72°C for 20 seconds. Fluorescence detection was performed at 72°C. The gene-specific primers were designed using the Primer3 software to amplify fragments of 150 to 250 bp as follows: for $D_2r$ (Drd2; NM 010077) forward, TCGCCATTGTCTGGGTCCTG; reverse, TGCCCTTGAGTGGTGTCTTC; and $D_1r$ (Drd1a; NM 010076) forward, AAGATGCCGAGGATGACAAC; reverse, CCCTCTCCAAAGCTGAGATG. The transcript amounts that were evaluated for the $D_1rs$ and $D_2rs$ were normalized for quantity and quality of each sample by dividing it by the amount of transcript of the housekeeping gene acidic ribosomal phosphoprotein P0 (Arbp or 36B4; NM 007475) in the same sample, and their relative values were presented. The 36B4 transcript amount was quantified using the forward primer ACCCTGAAGTGCTCGACATC and reverse primer AGGAAGGCCTTGACCTTTTC.

## Immunohistochemistry

Coronal sections (14 μm thick) from the unfixed frozen brains of mice were collected on superfrost slides and stored at –80°C until analysis. The sections were postfixed in 4% paraformaldehyde and treated with 1% $H_2O_2$ to block endogenous peroxides. For the detection of $D_2rs$, the primary antibody was detected using the ABC system (Vector) according to the manufacturer's manual. For each animal and section, the corresponding brain regions were identified according to the mouse brain atlas (Franklin and Paxinos, 2008).

## Locomotor Activity

Mice were individually placed in a transparent acrylic cage with a black frosting Plexiglas floor (45 × 25 × 40 cm), and locomotor activity was measured every 5 minutes for 60 minutes using digital counters with infrared sensors (Scanet MV-40; MELQEST, Toyama, Japan). METH (1 mg/kg subcutaneously [s.c.]) was administered immediately before the measurement of locomotor activity.

## Place Conditioning Test

A place conditioning test was performed according to the method of Miyamoto et al. (2000). In brief, the apparatus consisted of the following 2 compartments: transparent and black Plexiglas boxes (both 15 × 15 × 15 cm). The floors of the transparent and black boxes were covered with white and black frosting Plexiglas, respectively. Each box could be divided by a sliding door (10 × 15 cm high). In preconditioning, the sliding door was opened, and the mouse was allowed to move freely between both boxes for 15 minutes once per day for 3 days. On day 3, the time that the mouse spent in the transparent and black boxes was measured using a LD mode of Scanet MV-40 (MELQEST). The box in which the mouse spent the most time was referred to as the "preferred side" and the other box was the "nonpreferred side." The conditioning was performed during 6 successive days. The mouse was given a drug or vehicle immediately before the conditioning in the apparatus with the sliding door closed. On days 4, 6, and 8, the mouse was given METH (1 mg/kg s.c.) or saline and placed in its nonpreferred side for 20 minutes. On days 5, 7, and 9, the mouse was given saline and placed in its preferred side (opposite to the METH-conditioning side) for 20 minutes. On day 10, postconditioning was performed without drug treatment. During postconditioning, the sliding door was opened, and the time that the mouse spent in the transparent and black boxes for 15 minutes was measured as on day 3. Place conditioning behavior was expressed by post – pre, which was calculated as follows: [(post value) – (pre value)], where the post and pre values were the differences in the time spent in the METH-conditioning and saline-conditioning sides in postconditioning and preconditioning, respectively.

## Western-Blotting Analysis

The brain tissues of the NAc core were homogenized in a lysis buffer (50 mM Tris-HCl, pH 7.5, 150 mM NaCl, 5 mM ethylenediaminetetraacetic acid, 1% Triton X-100, 0.5% sodium deoxycholate, 1 mM phenylmethylsulfonyl fluoride, phosphatase inhibitor cocktail [Nacalai Tesque, Kyoto, Japan] and protease inhibitor cocktail [Nacalai Tesque]). Total proteins (20 μg) were separated by sodium dodecyl sulfate-polyacrylamide gel electrophoresis and blotted onto a polyvinylidene difluoride membrane. The membranes were incubated with primary antibodies, and the proteins were detected by horseradish peroxidase-conjugated secondary antibodies using the ECL Plus detection kit (Amersham Biosciences).

## Statistical Analysis

All experiments were repeated twice with independently generated mice. All data are expressed as the mean ± SEM. In the analysis of locomotor activity and the place conditioning test, statistical differences among values for individual groups were determined using an analysis of variance (ANOVA) followed by the Student–Newmann–Keuls multiple comparisons test when $F$ ratios were significant ($P < .05$). In the analysis of the time course of the development of locomotor sensitization, statistical differences were determined using ANOVA with repeated measures. Statistical differences between 2 groups were determined with the Student's $t$ comparison test.

# Results

## Reduced $D_2rs$ in the Nucleus Accumbens of $miD_2r$ Mice

First, we examined the mRNA expression levels of $D_2rs$ and $D_1rs$ in the NAc and dSTR of $miD_2r$ mice. Real-time quantitative

reverse transcription-PCR (RT-PCR) revealed a significant reduction (47%) in $D_2r$ mRNA expression levels in the NAc of $miD_2r$ mice compared with those in the control Mock mice (Figure 1A). However, there was no reduction in $D_1r$ mRNA expression levels in the NAc of $miD_2r$ mice (Figure 1A). Furthermore, in the dSTR, both $D_2r$ and $D_1r$ mRNA expression levels were not significantly different between Mock and $miD_2r$ mice (Figure 1A). Consistent with the above $D_2r$ mRNA expression levels, the protein expression levels of the $D_2rs$ using Western blotting and immunochemical staining were diminished in the core region of the NAc of $miD_2r$ mice (Figure 1B-C). Supporting that, the expression of GFP was observed in the SNr, but not in the VTA, in both mice (Figure 1D), because the SNr receives axial projection from the core region, but not the shell region, of the NAc (Humphries and Prescott, 2010). These findings suggest that $miD_2r$ mice have half reduction, but not a complete loss, of $D_2rs$ in the core region of the NAc.

## Attenuated METH-Induced Locomotor Activity and Place Preference in $miD_2r$ Mice

To investigate whether the specific reduction of $D_2rs$ in the NAc of mice affects the CNS functions of the brain, we examined the performances of $miD_2r$ mice in several behavioral paradigms. We first tested their motility in a novel environment as a general behavioral response, which was measured for horizontal activity (locomotion) after saline treatment. No aberrant locomotion during a 60-minute observation period was seen in $miD_2r$ mice (Figure 2A). This result indicates no apparent abnormalities in the motor neuronal systems of $miD_2r$ mice. Acute METH (1 mg/kg s.c.) treatment induced hyperlocomotion in both Mock and $miD_2r$ mice. However, the magnitude of the METH-induced

locomotor activity in $miD_2r$ mice was significantly reduced compared with that in Mock mice (Figure 2A). In both groups, the hyperlocomotion was potentiated by repeated METH treatment (1 mg/kg/d s.c.) for 7 days. When the time course of the METH-induced locomotor sensitization in $miD_2r$ mice was compared with that in Mock mice, the development of sensitization was found to be significantly less extensive in the knockdown mice, at 1 mg/kg/d of METH [Figure 2B: ANOVA with repeated measurement; $F_{(1, 12)} = 4.908, P = .035$].

In the place conditioning test, METH (1 mg/kg s.c.) significantly induced place preference in both Mock and $miD_2r$ mice. However, the preferred effects of METH were significantly weaker in $miD_2r$ mice than in Mock mice (Figure 3).

## Decreased METH-Induced ERK and CREB Phosphorylation and Delta FosB Accumulation in the Core of the NAc of $miD_2r$ Mice

Subsequently, we investigated the intracellular signal responses to METH in the core of the NAc of $miD_2r$ mice. Acute METH treatment (1 mg/kg s.c.) increased the phosphorylation levels of ERK at Threonine 202/Tyrosine 204 and CREB at Serine 133 in Mock mice (Figure 4A-B). However, the METH-induced phosphorylation levels of ERK and CREB in $miD_2r$ mice showed a significant decrease compared with those in Mock mice (Figure 4A-B). A previous report demonstrated that chronic treatment of addictive drugs results in the accumulation of transcription factor delta FosB, which is mediated by CREB activation in the NAc (Kelz et al., 1999). The expression levels of delta FosB in the normal condition were the same in both $miD_2r$ and Mock mice (Figure 4C). Repeated METH treatment increased the expression levels of delta FosB in Mock mice (Figure 4C). However, this
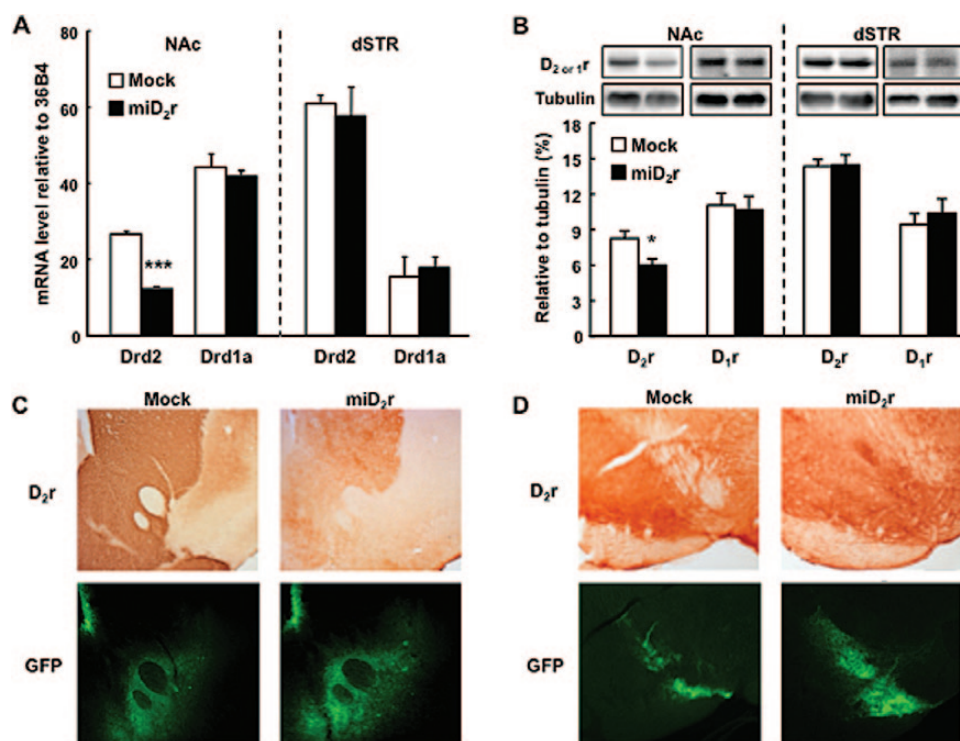


**Figure 1.** Expression of dopamine $D_2$ receptor ($D_2r$) in the nucleus accumbens (NAc) of the adeno-associated virus vectors containing a microRNA sequence for D2r-treated mice ($miD_2r$ mice). A, Expression level of *Drd2* or *Drd1a* mRNA was measured by quantitative reverse transcription-polymerase chain reaction and presented relative to the expression of *36B4*. B, Expression level of $D_2r$ or dopamine $D_1$ receptor ($D_1r$) protein was assessed by Western blotting. C, Immunohistochemical study of the $D_2r$ and green fluorescent protein (GFP) in the NAc of $miD_2r$ mice. D, Immunohistochemical study of the $D_2r$ and GFP in the substantia nigra pars reticulata (SNr) of $miD_2r$ mice. dSTR, dorsal striatum. N = 6. Each column represents the mean ± SEM. *P < .05, ***P < .001 vs Mock mice (Student's t comparison test).
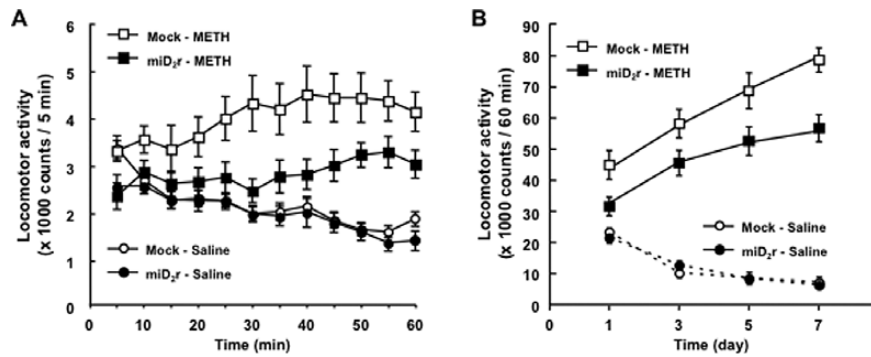
**Figure 2.** Locomotor effects of methamphetamine (METH) in $miD_2r$ mice. A, Locomotor activity induced by acute METH treatment. METH (1 mg/kg s.c.) was administered immediately before the measurement of locomotor activity every 5 minutes for 60 minutes. N=7. Analysis of variance (ANOVA) with repeated-measurement analysis; $F_{(1, 12)}$=6.969, P=.001. B, Locomotor sensitization induced by repeated METH treatment. METH (1 mg/kg/d s.c. for 7 days) was administered to the mice that were used in A. The development of sensitization was found to be significantly lower in $miD_2r$ mice. N=7. ANOVA with repeated-measurement analysis; $F_{(1, 12)}$=4.908, P=.035.
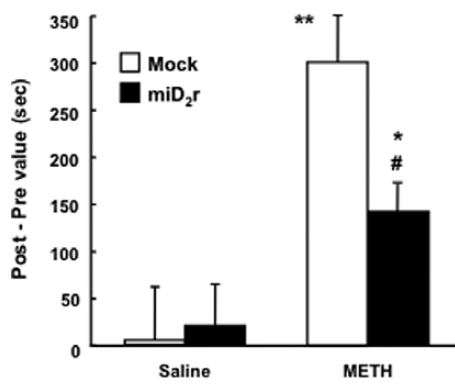


**Figure 3.** Preferred effects of methamphetamine (METH) in $miD_2r$ mice. Place preference induced by METH treatment. METH (1 mg/kg s.c.) was administered during the conditioning. N=8. Each column represents the mean±SEM. *P<.05, **P<.01 vs corresponding saline-treated group. #P<.05 vs corresponding Mock group.

METH-induced expression of delta FosB in $miD_2r$ mice showed a significant attenuation compared with that in Mock mice (Figure 4C).

## Discussion

AAV vectors are powerful tools for delivering an objective gene into the neurons because of its unique characteristics, including the lack of any disease caused by wild-type viruses, the ability to infect nondividing cells, and the long-term expression of the transgene without immune responses (Monahan and Samulski, 2000). In the present study, we constructed the AAV vectors containing the miRNA sequence for $D_2r$ and GFP as a vector-working marker and microinjected those into the NAc of mice. The AAV-$miD_2r$ vectors selectively controlled the expression levels of $D_2rs$ without affecting those of $D_1rs$. Furthermore, the expression of GFP was observed in the NAc and SNr but not in the dSTR and VTA. These findings suggest that the postsynaptic but not the presynaptic (axon terminals of afferent fibers) $D_2rs$ on the DAergic synapses in the core of the NAc were reduced by the delivery of the AAV-$miD_2r$ vectors. Therefore, the $miD_2r$ mice would exhibit dysfunction of the indirect γ-aminobutyric acidergic pathway projecting to the SNr from $D_2rs$-expressing MSNs in the core of the NAc.

METH increases the extracellular levels of DA by modulating its release and reuptake and thereby acts as an indirect agonist for DA receptors. METH induces abnormal behaviors, such as hyperlocomotion, locomotor sensitization, and conditioned place preference. Furthermore, METH leads to altered intracellular signal transduction, such as induction of the transcription factors CREB and delta FosB. In our results, the METH-induced behavioral and intracellular signal impairments were partially improved in $miD_2r$ mice. This observation appeared to be consistent with previous results that have been obtained from some pharmacological experiments with $D_2r$ antagonists to investigate the mechanisms of METH-induced rewarding effects (Mizoguchi et al., 2004; Carati and Schenk, 2011; Kurokawa et al., 2012). However, considering the defective selectivity to the target molecules in the chemical compounds that are so-called selective $D_2r$ antagonists and the expression of $D_2rs$ on both presynaptic and postsynaptic sides of the DAergic synapses, the pharmacological blockade of $D_2rs$ was insufficient to explain in detail the contribution of $D_2r$ in METH-induced addiction. In contrast, our observation precisely indicates that the indirect pathway from $D_2rs$-expressing MSNs in the NAc plays an important role in the development of addictive responses.

However, there have been many reports of the pharmacological experiments in which $D_1r$ antagonists attenuate abnormal behaviors and alter the intracellular signaling that is induced by drugs of abuse, including METH. Furthermore, recent reports demonstrated that the specific cells expressing $D_1rs$ in the STR, including the NAc, play a role in addictive behaviors induced by repeated exposures to cocaine (Hikida et al., 2010; Kim et al., 2011), that is, these demonstrations propose that the direct pathway from MSNs that express $D_1rs$ plays an important role in the development of addiction, and these were different from our observations. This contradiction may be explained by the hypothesis that there is a different neural circuit in distinct situations of drug addiction. The reinforcing effects of addictive drugs engage reward neurotransmitters and associative mechanisms in the VTA-NAc, and stimulus–response habits depend on the SN-dSTR (reviewed in Koob and Volkow, 2010). Therefore, although the NAc and dSTR constitute a similar cell population and output pathway, these brain regions serve different aspects in each situation of drug addiction through distinct neuronal inputs. For other causes, it has been reported that there are approximately 1 to 2% of spiny large cholinergic interneurons in the NAc. Therefore, the MSNs that express $D_1rs$ and $D_2rs$ may have direct or indirect reciprocal interactions in the core of the NAc, and the cholinergic interneurons in the NAc play an important role in the cocaine reward system (Hikida et al., 2003). Thus, the above findings and our observations suggest that the cholinergic interneurons expressing $D_2rs$ modulate
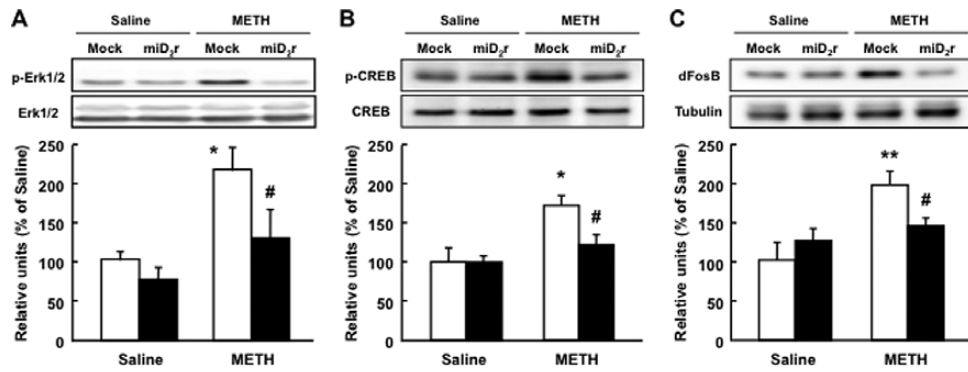
**Figure 4.** Intracellular effects of methamphetamine (METH) in miD$_2$r mice. A, METH-induced extracellular signal regulated kinase (ERK2) phosphorylation in miD$_2$r mice. B, METH-induced cAMP response element-binding protein (CREB) phosphorylation in miD$_2$r mice. Mice were treated once with METH (1 mg/kg) and sacrificed 15 minutes later. N = 4. *$P < .05$, **$P < .01$ vs saline, #$P < .05$ vs Mock (Student–Newmann–Keuls test). C, METH-induced deltaFosB expression in miD$_2$r mice. Mice were repeatedly treated with METH (1 mg/kg/d for 7 days). N = 4. **$P < .01$ vs saline, #$P < .05$ vs Mock (Student–Newmann–Keuls test).

the direct pathway from the MSNs expressing D$_1$rs in the core of the NAc. In any case, for the elucidation of the neural networks in the core of the NAc, further examinations using the cell-type and regional-specific gene modification technologies are necessary.

In summary, our observations exhibited the usefulness of AAV-miD$_2$r vectors as a gene therapy tool for the purposed functional inhibition of D$_2$rs in patients with DA-related symptoms. In addition, the knockdown of D$_2$rs in the core of the NAc suppresses reinforcement-related behavioral and intracellular responses induced by addictive drugs.

## Statement of Interest

None.

## References

Carati C, Schenk S (2011) Role of dopamine D1- and D2-like receptor mechanisms in drug-seeking following methamphetamine self-administration in rats. Pharmacol Biochem Behav 98:449–454.

Franklin KBJ, Paxinos G (2008) In: The mouse brain in stereotaxic coordinates. 3rd ed. New York: Academic Press.

Gerfen CR, Surmeier DJ (2011) Modulation of striatal projection systems by dopamine. Annu Rev Neurosci 34:441–466.

Groenewegen HJ, Wright CI, Beijer AV, Voorn P (1999) Convergence and segregation of ventral striatal inputs and outputs. Ann N Y Acad Sci 877:49–63.

Hikida T, Kitabatake Y, Pastan I, Nakanishi S (2003) Acetylcholine enhancement in the nucleus accumbens prevents addictive behaviors of cocaine and morphine. Proc Natl Acad Sci USA 100:6169–6173.

Hikida T, Kimura K, Wada N, Funabiki K, Nakanishi S (2010) Distinct roles of synaptic transmission in direct and indirect striatal pathways to reward and aversive behavior. Neuron 66:896–907.

Humphries MD, Prescott TJ (2010) The ventral basal ganglia, a selection mechanism at the crossroads of space, strategy, and reward. Prog Neurobiol 90:385–417.

Hyman SE, Malenka RC, Nestler EJ (2006) Neural mechanisms of addiction: the role of reward-related learning and memory. Annu Rev Neurosci 29:565–598.

Kelz MB, Chen J, Carlezon WA Jr, Whisler K, Gilden L, Beckmann AM, Steffen C, Zhang YJ, Marotti L, Self DW, Tkatch T, Baranauskas G, Surmeier DJ, Neve RL, Duman RS, Picciotto MR, Nestler EJ (1999) Expression of the transcription factor deltaFosB in the brain controls sensitivity to cocaine. Nature 401:272–276.

Kim J, Park BH, Lee JH, Park SK, Kim JH (2011) Cell type-specific alterations in the nucleus accumbens by repeated exposures to cocaine. Biol Psychiatry 69:1026–1034.

Koob GF, Volkow ND (2010) Neurocircuitry of addiction. Neuropsychopharmacology 35:217–238.

Kreitzer AC, Malenka RC (2008) Striatal plasticity and basal ganglia circuit function. Neuron 60:543–554.

Krzyzosiak A, Szyszka-Niagolov M, Wietrzych M, Gobaille S, Muramatsu S, Krezel W (2010) Retinoid x receptor gamma control of affective behaviors involves dopaminergic signaling in mice. Neuron 66:908–920.

Kurokawa K, Mizuno K, Ohkuma S (2012) Possible involvement of type 1 inositol 1,4,5-trisphosphate receptors up-regulated by dopamine D1 and D2 receptors in mouse nucleus accumbens neurons in the development of methamphetamine-induced place preference. Neuroscience 227: 22–29.

Li XG, Okada T, Kodera M, Nara Y, Takino N, Muramatsu C, Ikeguchi K, Urano F, Ichinose H, Metzger D, Chambon P, Nakano I, Ozawa K, Muramatsu S (2006) Viral-mediated temporally controlled dopamine production in a rat model of Parkinson disease. Mol Ther 13:160–166.

Lüscher C, Ungless MA (2006) The mechanistic classification of addictive drugs. PLoS Med 3:e437.

Missale C, Nash SR, Robinson SW, Jaber M, Caron MG (1998) Dopamine receptors: from structure to function. Physiol Rev 78:189–225.

Miyamoto Y, Noda Y, Komori Y, Sugihara H, Furukawa H, Nabeshima T (2000) Involvement of nitric oxide in phencyclidine-induced place aversion and preference in mice. Behav Brain Res 116:187–196.

Mizoguchi H, Yamada K, Mizuno M, Mizuno T, Nitta A, Noda Y, Nabeshima T (2004) Regulations of methamphetamine reward by extracellular signal-regulated kinase 1/2/ets-like gene-1 signaling pathway via the activation of dopamine receptors. Mol Pharmacol 65: 1293–1301.

Monahan PE, Samulski RJ (2000) AAV vectors: is clinical success on the horizon? Gene Ther 7:24–30.

Stoof JC, Kebabian JW (1981) Opposing roles for D-1 and D-2 dopamine receptors in efflux of cyclic AMP from rat neostriatum. Nature 294:366–368.